Semi-active H∞/LPV control for an industrial hydraulic damper

Sébastien Aubouet, Luc Dugard, Olivier Sename, Charles Poussot-Vassal, Benjamin Talon

Semi-active $\mathcal{H}_\infty/LPV$ control for an industrial hydraulic damper

S. Aubouet[1,2] and L. Dugard[1] and O. Sename[1] and C. Poussot-Vassal[1] and B. Talon[2]

***Abstract*— In this paper, a new control strategy is developed to improve comfort and roadholding of a ground vehicle equipped with an industrial damper. This damper can be controlled by means of a small servomechanism which adjusts the damping rate. The main controller is a linear parameter varying (LPV) static state-feedback controller synthesized in the $\mathcal{H}_\infty/LPV$ framework to compute the required damping force that minimizes the movements of the vehicle's body on one hand, and the deflection of the tire on the other hand. A scheduling strategy is developed on the basis of the real damper behavior to improve performances without using active damping forces which would be useless for such a semi-active system. Here the controller takes the constraints of the technology and the damper behavior into account and is easy to implement in an industrial application. The control of the servomechanism is provided by a simple PID controller that ensures that the damper provides the required force. The performances are illustrated on an identified nonlinear model of the damper embedded in a quarter car model. The comfort and roadholding level of the semi-active suspension are studied using some adapted criteria and compared with the passive ones. Some simulations emphasize the comfort and roadholding improvements of this control stategy that will be tested by SOBEN on a testing car in the near future.**

I. INTRODUCTION

The main role of suspensions is to improve comfort by isolating the vehicle chassis from an uneven ground and providing a good roadholding to ensure the safety of the passengers, especially during a bend. Suspension control based on quarter vehicles has been widely explored in the past few years to improve vertical movements. Active control laws have been developed: Skyhook [13], [5], $\mathcal{H}_\infty$ control [7], LPV [6] or mixed synthesis [1], [19], and semi-active control laws [18], [20], [9] using a mix one-sensor control strategy [14], model predictive techniques [4], [8] and quasi-linearization and frequency shaping [10]. Semi-active suspensions are very interesting because of their low energy consumption when compared to active ones and their high performances when compared to passive ones.

The contribution of this paper is a semi-active control stategy that optimizes the vehicle behavior considering the constraints of the actuator and the damper behavior in the controller. A semi-active suspension control strategy based on $\mathcal{H}_\infty/LPV$ techniques has already been developed in [12]. Here this previous study is completed: the performance specifications are scheduled, and the damper limitations are determined using identified models. Finally, an efficient and complete industrial solution including a high-level controller and a low-level force control-loop is proposed.

This paper is organized as follows: the SOBEN damper and its actuator are described and modelled in Section II. In Section III, the control strategy is developed. In Section IV, some simulation results are given in time and frequency and show the interest of semi-active suspensions when compared with passive ones. This paper is concluded in Section V and finally, some possible future works are proposed.

II. PRESENTATION AND MODELLING OF SOBEN DAMPER

A. SOBEN damper

The system under study is the semi-active hydraulic damper designed by SOBEN and represented on Figure 1. The oil flow in the damper is controlled with a single servomechanism. This actuator is also represented on Figure 1.

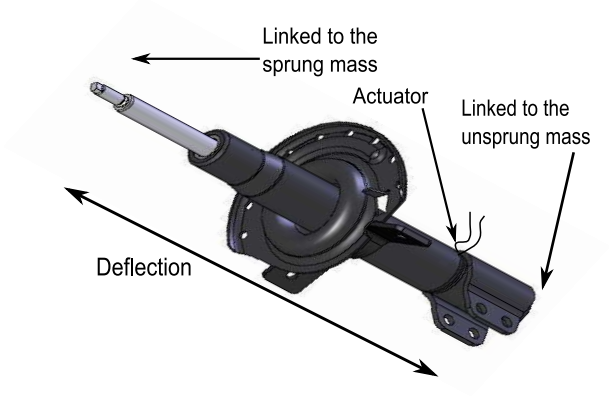

Fig. 1. New SOBEN damper

Some experiments have been done with SOBEN's testing bench. Different sinusoidal excitations have been applied to the damper with varying amplitudes and frequencies. The damping force and the deflection are measured and represented on a so called force-deflection diagram.

These experiment results have been used to identify a simplified model of the damper given by Equation 1. This model has been proposed by [17] for magneto-rehological dampers. This is a static nonlinear model that gives the damping force using the deflection and deflection speed. Here this model has been applied to an hydraulic damper with a high hysteretic behavior: the force does not only depend on the deflection speed, it also depend on the

[1]GIPSA-lab, Control Systems Departement, ENSIEG, Domaine Universitaire, 38402 Saint-Martin d'Hères, FRANCE, olivier.sename@inpg.fr, luc.dugard@inpg.fr.fr

[2]SOBEN S.A.S., Pôle Mécanique d'Alès Cévenes, Vallon de Fontanes, 30520 St-Martin de Valgalgues, FRANCE, sebastien.aubouet@soben.fr

deflection. Therefore this hysteresis can be modelled by the following simple model:

$$F_s = A_1 \tanh(A_2 v + A_3 x) + A_4 v + A_5 x \qquad (1)$$

where F_s is the damping force, v is the deflection speed, x is the deflection and A_i, $i \in [1,5]$ are the identified parameters.

The experiment results used to identify the damper are a set of sinusoidal deflections: amplitude $1.5, 3.5, 5, 7.5, 8.5mm$ with a frequency of $12Hz$ and amplitude $2, 7, 12, 18mm$ with a frequency of $1.5Hz$. The optimization has been done on the whole experiment set in order to identify an accurate model in high frequencies ($12Hz$) as well as in low frequencies ($1.5Hz$). An identification algorithm solving the nonlinear data-fitting problem in the least squares sens has been used to identify the model given in Equation 1.

The performances of the identified model have been tested with another set of experiments, with different sinusoidal deflections: amplitude $1, 2, 3, 6mm$ with a frequency of $12Hz$ and amplitude $3, 6, 11, 16mm$ with a frequency of $1.5Hz$. The measured force-deflection diagrams are compared with the simulated force-deflection diagrams on Figure 2. The accuracy of the identified model is shown on this diagram, because the curves are almost superposed.

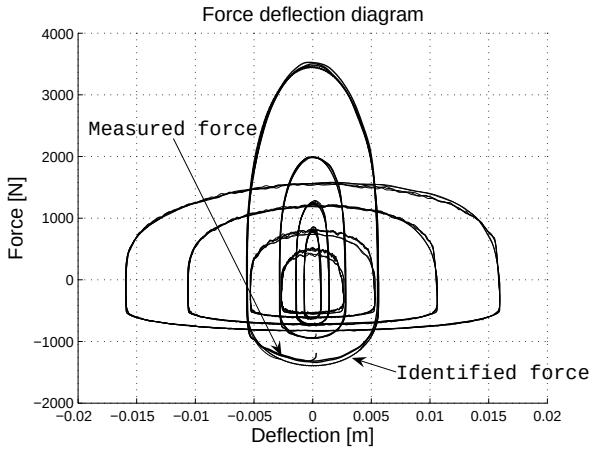

Fig. 2. Measured and identified damping force

This model will be used by the high-level controller to compute a realistic required damping force taking the behavior of the damper into account.

B. Actuator

The actuator chosen for SOBEN damper is the flow control solenoide valve represented on Figure 3. The oil flow in the damper at a given deflection speed can be controlled by changing the input current of the servomechanism.

The step response of the actuator shows that the system behaves like a simple second order with the current as input and the oil flow as output. The bandwidth ω_0 and the damping coefficient m have been deduced from this step response. Moreover the experiments show that controlling the flow in the damper is equivalent to controlling the damping rate C ($N \cdot s/m$) of the damper. For a given excitation signal and a varying input current, the average slope of the force-speed diagram gives the damping rate. Therefore C has been directly identified on the experiment results. It corresponds to the linear static gain G of the actuator model G_{act} given by Equation 2. The input is the current I and the output is the damping rate C.

$$G_{act}(s) = \frac{C(s)}{I(s)} = \frac{G}{(\frac{s}{\omega_0})^2 + 2m\frac{s}{\omega_0} + 1} \qquad (2)$$

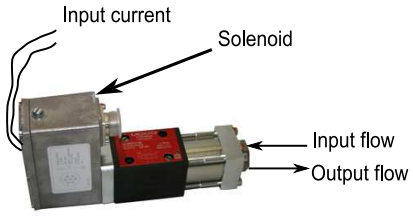

Fig. 3. Servomechanism

This actuator has been chosen for its dimensions and resistance to high pressures. Here one of the objectives was to simulate the complete system and check the compatibility of this actuator with the developed control strategies.

The actuator presented on Figure 3 and modelled by Equation 2 provides the damping rate C that corresponds to A_4 in the identified model. Therefore the semi-active damper can be modelled as:

$$F_s = A_1 \tanh(A_2 v + A_3 x) + Cv + A_5 x \qquad (3)$$

where C is given by Equation 2.

C. Vehicle model

The vehicle model used in this paper is a vertical linear quarter car model represented on Figure 4. The identified damper model given by Equation 3 has been embedded in the quarter car model.

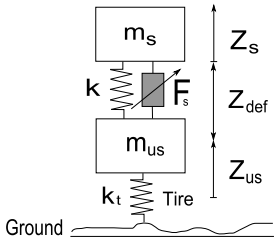

Fig. 4. Vertical quarter car vehicle

The equations of this model are given by Equation 4.

$$\begin{cases} m_s \ddot{z}_s = k(z_{us} - z_s) + F_s \\ m_{us} \ddot{z}_{us} = k(z_s - z_{us}) - F_s + k_t(z_r - z_{us}) \end{cases} \qquad (4)$$

TABLE I

QUARTER CAR PARAMETERS AND VARIABLES

m_s, m_{us}	Sprung, unsprung mass
k, k_t	Suspension, tire stiffness
z_r	Ground vertical position
$\ddot{z}_s$, $\ddot{z}_{us}$	Sprung, unsprung mass acceleration
z_s, z_{us}	Sprung, unsprung mass position
$z_{def} = z_s - z_{us}$	Suspension deflection
F_s	Damping force

This model will be used later as reference model for simulations.

III. CONTROL ARCHITECTURE OF THE DAMPER

Here the controller developed to improve the vehicle performances aims at controlling the new semi-active SOBEN damper using a semi-active control strategy based on its real behavior.

A. Control strategy

The overall control architecture is presented on Figure 5. S_1 is the controlled model and includes the model of the quarter car, the nonlinear identified damper model and the model of the servomechnism given by Equation 3 and 4. S_2 is the observer designed by [21] and presented in Section III-B. This observer estimates the state variables $x = [z_s - z_{us}, \dot{z}_s, z_{us} - z_r, \dot{z}_{us}]^T$ of the quarter vehicle. The LPV static state-feedback force controller S_3 receives the observed state variables x as an input and gives the required damping force in order to improve the vehicle performances. This controller is scheduled by the parameter ρ that increases or decreases the performances required in such a way that the required force F^* is always semi-active and adapted to the actuator abilities. The controller S_4 computes the proper servomechanism input current that allows the damper to provide the required damping force F^*. This controller needs the real damping force F_{real} which is obtained using some measurements M and through a calculation procedure. This part is confidential due to patented results.

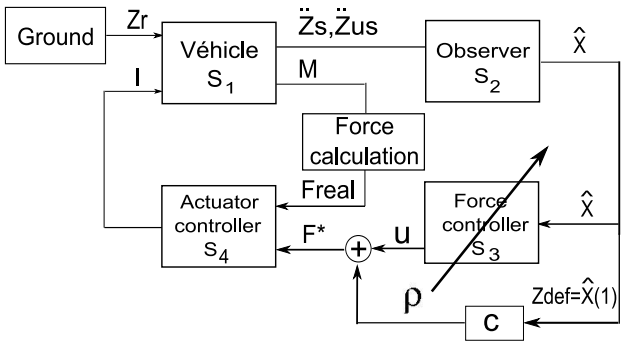

Fig. 5. Control architecture

B. State observer

A disturbance decoupled nonlinear state observer for a semi-active suspension has been designed by [21] assuming that the sprung mass and unsprung mass accelerations are measured. These signals are available in the application considered here. u is the controllable damping rate of the suspension, $w = \dot{z}_r$ the rate of road elevation change (unknown input) and $\hat{x} = [z_s - z_{us}, \dot{z}_s, z_{us} - z_r, \dot{z}_{us}]^T$ the state variables vector of the following nonlinear system to be observed:

$$\dot{\hat{x}} = A \cdot \hat{x} + D \cdot \hat{x} \cdot u + R \cdot w,$$

$$A = \begin{pmatrix} 0 & 1 & 0 & -1 \\ -\frac{k}{m_s} & 0 & 0 & 0 \\ 0 & 0 & 0 & 1 \\ \frac{k}{m_{us}} & 0 & -\frac{k_t}{m_{us}} & 0 \end{pmatrix},$$

$$D = \begin{pmatrix} 0 & 1 & 0 & 0 \\ 0 & -\frac{1}{m_s} & 0 & \frac{1}{m_s} \\ 0 & 0 & 0 & 1 \\ 0 & \frac{1}{m_{us}} & 0 & -\frac{1}{m_{us}} \end{pmatrix},$$

$$R = \begin{pmatrix} 0 & 0 & -1 & 0 \end{pmatrix}^T$$

The non linear observer has been designed such that:

- The estimation error is not affected by the unknown road disturbance,
- The observation error on the deflection and deflection speed are exponentially stable,
- The sprung and unsprung masses are estimated without the effects of D.C. offsets.

$$\dot{z} = \begin{pmatrix} A_1 & O & O & O \\ A_2 & O & O & O \\ O & C_1 & A_3 & O \\ A_2 & C_2 & O & A_3 \end{pmatrix} \cdot z + \begin{pmatrix} B_1 & O \\ B_2 & O \\ O & O \\ O & O \end{pmatrix} \cdot z \cdot u + \begin{pmatrix} L \\ O \end{pmatrix} (y_1 - \hat{y}_1) + \begin{pmatrix} M \\ O \end{pmatrix} y_2$$

$$\hat{y}_1 = \frac{k}{m_s} z_1 - \frac{1}{m_s} z_2 \cdot u$$

$$\hat{x} = \begin{pmatrix} I_{4,4} & A_4 \\ T_1 & O \end{pmatrix} \cdot z + \begin{pmatrix} O & O \\ T_2 & O \end{pmatrix} \cdot z \cdot u + \begin{pmatrix} O \\ -\frac{m_{us}}{k_t} \end{pmatrix} y_2$$

where:

$$A_1 = \begin{pmatrix} 0 & 1 \\ -\frac{k}{m_s} & 0 \end{pmatrix}, A_2 = \begin{pmatrix} -\frac{k}{m_s} & 0 \\ 0 & 0 \end{pmatrix},$$

$$B_1 = \begin{pmatrix} 0 & 0 \\ 0 & -\frac{1}{m_s} \end{pmatrix}, B_1 = \begin{pmatrix} 0 & -\frac{1}{m_s} \\ 0 & 0 \end{pmatrix},$$

$$C_1 = \begin{pmatrix} I & 0 \\ 0 & 0 \end{pmatrix}, C_2 = \begin{pmatrix} 0 & I \\ 0 & 0 \end{pmatrix},$$

$$A_3 = \begin{pmatrix} -a_1 & -a_2 \\ 0 & 0 \end{pmatrix}, A_4 = \begin{pmatrix} 0 & 0 & 0 & 0 \\ 0 & 0 & 0 & 0 \\ -a_1 & -a_2 & 0 & 0 \\ 0 & 0 & -a_1 & -a_2 \end{pmatrix},$$

$$M = \begin{pmatrix} 0 & -1 & 0 & 1 \end{pmatrix}^T, T_1 = \begin{pmatrix} \frac{k}{k_t} & 0 & 0 & 0 \end{pmatrix}^T,$$

$$T_2 = \begin{pmatrix} 0 & \frac{1}{k_t} & 0 & 0 \end{pmatrix}^T, a_1 = c_b, a_2 = \omega_c^2,$$

ω_c: cutoff frequency, c_b: filter constant, O: is the null matrix with proper dimension and L is the observer gain.

For more details about the synthesis and the performances of this observer, see [21].

C. $\mathcal{H}_\infty/LPV$ force controller

The $\mathcal{H}_\infty$ approach is interesting to tackle frequency specifications. Here the objective is to minimize the four transfer functions $\ddot{z}_s/z_r$, z_s/z_r (comfort), z_{us}/z_r and z_{def}/z_r (road-holding) at given frequencies. More details are given in a previous work [3]. LPV techniques can be used to schedule the controller according to measured varying parameters.

This has been used in [6], [12] to adapt the performances specifications and to improve the robustness of the controlled system in [22].

The solution proposed here aims at improving the four performances using a $\mathcal{H}_\infty/LPV$ controller with varying performance specifications. This work completes the preliminary results [12]. The controller has been synthesized using a linear quarter car and damper model. The scheduling parameter is computed according to the difference between the real damping force and the force the damper can actually provide, on the basis of identified models. This solution allows the controller S_3 presented on Figure 5, to compute a realistic and semi-active required force that the damper is able to provide, using an identified damper model. The performance objectives are adapted on-line to the damper abilities. The required force received by the actuator controller S_4 as an input is $F^* = u + C \cdot \dot{z}_{def}$, where the damping rate C can be seen as the average damping rate of the damper, and u as the added energy to achieve the varying performance, computed by the $\mathcal{H}_\infty/LPV$ force controller. The generalized parameter dependent plant $P(\rho)$ considered for the synthesis is given by Figure 6 and the equation bellow:

$$P(\rho): \begin{pmatrix} \dot{x} \\ z \\ y \end{pmatrix} = \begin{pmatrix} A(\rho) & B_1 & B \\ C_1 & D & E \\ C & F & O \end{pmatrix} \begin{pmatrix} x \\ w \\ u \end{pmatrix}$$

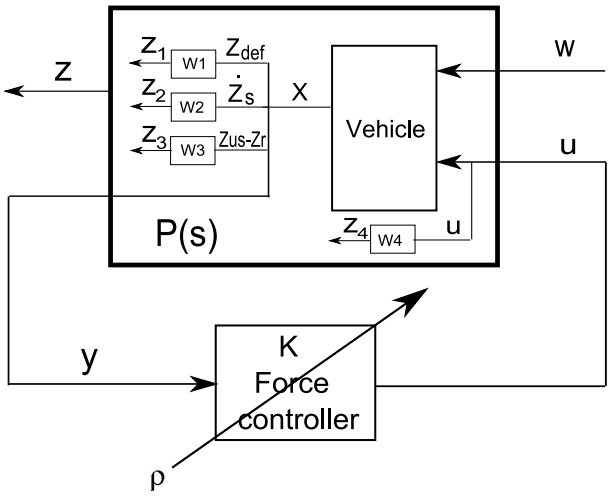

Fig. 6. Generalized plant and weighting functions

where the state variables vector $x = [x_{quarter}, x_{weighting}]$ includes the state variables vector of the quarter car (4) and the state variables vector of the weighting functions (performance specifications). $z = [z_1, z_2, z_3, z_4]$ are the weighed performance outputs to minimize, $y = \hat{x}$ is the observed state variables of the quarter car model, $w = \dot{z}_r$ is the ground variation and $\rho \in [0, \rho_{max}] = [0, 1]$ is the varying parameter used to schedule the controller. The weighting functions given by Equation 5 include the performance specifications detailed in [3].

$$\begin{cases} W_1(s)(\rho) = \frac{z_1}{z_{def}} = (\rho_{max} - \rho) \cdot \frac{G_1}{\frac{s}{2\pi f_{c_1}}+1} \\ W_2(s)(\rho) = \frac{z_2}{\dot{z}_s} = (\rho_{max} - \rho) \cdot \frac{G_2}{\frac{s}{2\pi f_{c_2}}+1} \\ W_3(s)(\rho) = \frac{z_3}{z_{us}} = (\rho_{max} - \rho) \cdot \frac{G_3}{\frac{s}{2\pi f_{c_2}}+1} \\ W_4(s)(\rho) = \frac{z_4}{u} = \rho \cdot \frac{G_4}{\frac{s}{2\pi f_{c_2}}+1}. \end{cases} \quad (5)$$

where $f_{c_1} = 1Hz$, $f_{c_2} = 20Hz$, $G_1 = 1$, $G_2 = 2$, $G_3 = 1$ and $G_4 = 1$.

The weighting functions W_1 and W_2 have been chosen to minimize the accelerations and vertical movements of the sprung mass in order to improve the comfort of the vehicle. W_3 and W_4 aim at reducing the tire and suspension deflections in order to reach a better roadholding. A scheduling strategy is proposed in [12] to avoid active forces by changing the weighting function of the control signal u. Here, the four weighting functions are scheduled by the parameter ρ which allows the performance objectives to be decreased if ρ is small, and increased if ρ is high. This parameter is computed according to (6) - (9).

$$\begin{cases} F_s^1 = A_1 \tanh(A_2 \dot{z}_{def} + A_3 z_{def}) + C_{min} \dot{z}_{def} + A_5 z_{def} \\ F_s^2 = A_1 \tanh(A_2 \dot{z}_{def} + A_3 z_{def}) + C_{max} \dot{z}_{def} + A_5 z_{def} \end{cases} \quad (6)$$

$$\begin{cases} F_s^{min} = \min(F_s^1, F_s^2) \\ F_s^{max} = \max(F_s^1, F_s^2) \end{cases} \quad (7)$$

$$F^* = \min(\max(F^*, F_s^{min}), F_s^{max}) \quad (8)$$

$$\rho = \frac{\min(\epsilon_{max}, \mid F_{real} - F^* \mid)}{\epsilon_{max}} \in [0, 1] \quad (9)$$

where ϵ_{max} is a given maximal force error.

In [12], the actuator constraints are only two extremal linear damping rates. Here ρ is evaluated using the identified damper model presented in Section II in order to determine the upper and lower reachable force obtained with the extremal outputs of the actuator: the extremal damping rates C_{min} and C_{max}. The reachable force range of the damper is represented on Figure 7. Zone 1 is active and unreachable, Zone 2 is semi-active but unreachable and Zone 3 is the reachable damper force range. The minimum and maximum of the extremal forces F_s^1 and F_s^2 computed in Equation 6 are determined with Equation 7 and used as limits for the saturation of the required force F^* given in Equation 8. Therefore this saturated required force is a reachable force reference. Then ρ is computed with Equation 9: $\rho = 0$ if $F_{real} = F^*$, $\rho = 1$ if $\mid F_{real} - F^* \mid > \epsilon_{max}$ and ρ is proportional to the force error if $\mid F_{real} - F_r \mid < \epsilon_{max}$. If $\rho = 0$ the weighting functions have small gains and the specified performances are the lowest. If $\rho = 1$ they are the highest. This solution allows the controller to decrease the performance objectives if the damper is not able to provide the required force.

The controller $K(\rho)$ synthesized is a LPV static state-feedback. Therefore with $u = K(\rho)x =$

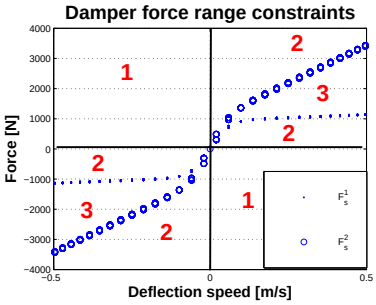

Fig. 7. Identified SOBEN damper force range

$K(\rho)[z_{def}, \dot{z}_s, z_{us} - z_r, \dot{z}_{us}]^T$, the closed-loop system is given by:

$$CL(\rho) = \begin{pmatrix} \dot{x} \\ z \end{pmatrix} = \begin{pmatrix} A(\rho)+BK(\rho) & B_1 \\ C+EK(\rho) & D \end{pmatrix} \begin{pmatrix} x \\ w \end{pmatrix}$$

The $\mathcal{H}_\infty$ problem consists in minimizing, or bounding to a given γ_∞ level, the system gain between $\|w\|_2$ and $\|z\|_2$ ($\mathcal{L}_2$ to $\mathcal{L}_2$ induced norm). The solution of this problem is given by the Bounded Real Lemma extended to LPV systems and the objective is to minimize γ_∞ such that:

$$\mathbf{X} = \mathbf{X}^T \succ 0, \mathbf{U} = K\mathbf{X}$$

$$\begin{pmatrix} \mathbf{X}A(\rho)^T + \mathbf{U}^T B + A(\rho)\mathbf{X} + B\mathbf{U} & B_1 & XC_1^T + \mathbf{U}^T E^T \\ B_1^T & -\gamma_\infty^2 I & D^T \\ C_1\mathbf{X} + E\mathbf{U} & D & -I \end{pmatrix} \prec 0$$

where the decision variables are X and U.

This inequality contains a parameter $\rho \in [\rho_{min}, \rho_{max}]$. Therefore this infinite set of LMI (Linear Matrix Inequality) established in [15], [16] has to be solved. The polytopic approach detailed in [2] consists in finding the unknown matrices X, U and a scalar γ_∞ that solve a finite set of LMI. This ensures the quadratic stability of the closed-loop system using a single Lyapunov function trough the evaluation of the previous LMI at each corner of the polytope only. This polytope is defined by the extremal varying parameters. Then the LPV controller is a linear combination of the controllers computed at each corner. Here there is only one parameter: $\rho \in [\rho_{min}, \rho_{max}]$. Thereafter, the controller is given by: $K = \rho \cdot K_{\rho_{min}} + (1-\rho) \cdot K_{\rho_{max}}$ where ρ_{min} and ρ_{max} define the corners of the polytope.

D. Servomechanism controller

Here the principle of the actuator controller S_4, represented on Figure 5, is briefly presented. Using the real damping force F_{real}, the required force F^* and the observed deflection speed z_{def}, the damping rate error ϵ_c is computed by $SS1$, represented on Figure 8. Then the servomechanism input current I is computed by a simple PID controller with high frequency filter and integral term saturation to control the damping rate. This PID controller has to be at least ten times faster than the force controller given in Section III-C.

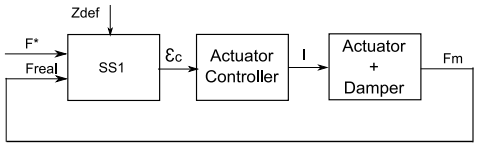

Fig. 8. Servomechanism control architecture

IV. SIMULATION RESULTS

In this section, some simulation results are given and show the interest of the semi-active control proposed in this paper. The quarter car model given by Equation 4, and the model of the damper with the actuator given by Equation 3 are used as a reference model for the following simulations.

Here the performances obtained are analysed using the pseudo-Bode diagrams presented on Figure 9. The methodology to compute these diagrams is detailed in [3], [11].

The following systems are compared on Figure 9:

- Passive linear damper with low damping rate: $C = 1500Ns/m : P_1$,
- Passive linear damper with high damping rate: $C = 3000Ns/m : P_2$,
- Semi-active damper with LPV control proposed in Section III-C,
- Semi-active damper with ADD control (Acceleration Driven Damper).

The ADD semi-active control uses the measurement of the sprung mass acceleration and the measurement of the deflection. This control law is detailed in [14] and has been used in this paper for comparison. The comfort level of the vehicle has been increased by the controller proposed in this paper and by the ADD controller, but the roadholding is better with the LPV solution. The results are very satisfying when compared to the passive dampers. They are also better than the semi-active ADD comfort oriented control which dammages the roadholding. Moreover the solution proposed is adjustable: the weighting functions are chosen, and the actuator bandwidth is considered in the controller. This is not possible with the ADD controller.

Consider now some time results presented on Figure 10 where the quarter car model has been submitted to a given random ground profile.

The accelerations of the sprung masses represented on Figure 10 show that the comfort levels of LPV, P_1, ADD are equivalent to each other and better than P_2. Therefore the accelerations are well minimized by the semi-active suspensions. The tire deflections graph shows that the roadholding of P_1 is the worth. Then LPV and P_2 are equivalent to each other and a bit better than ADD. Time and frequency results are coherent. The force-speed diagram given on Figure 10 shows that the force provided and required are not always semi-active. This is due to the fact that the constraints are based on an identified damper model that models the hysteresis of the real damper. Therefore the hysteresis is allowed by the controller when this hysteresis is realistic. Furthermore the figure shows that the required force and

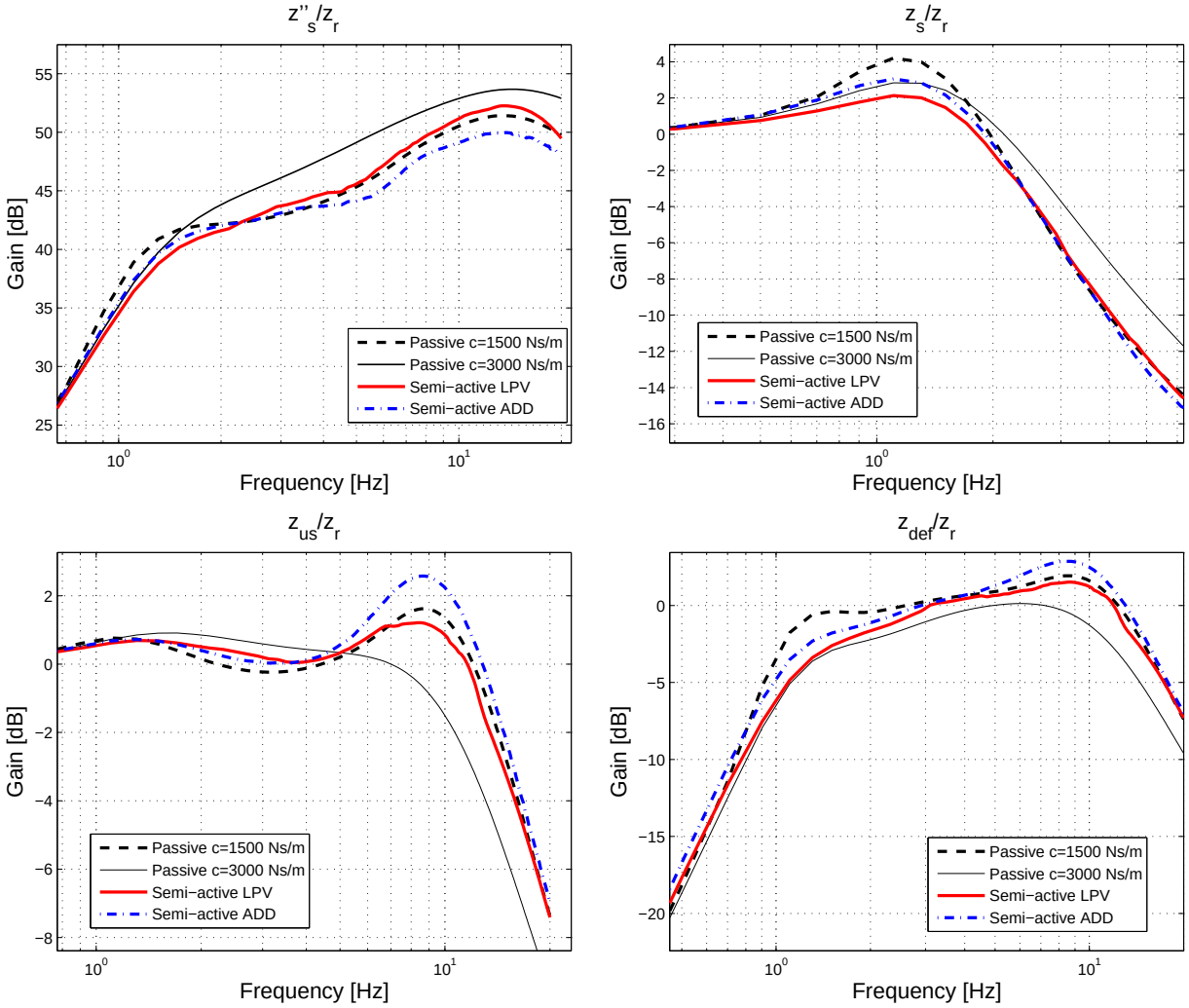

Fig. 9. Frequency results

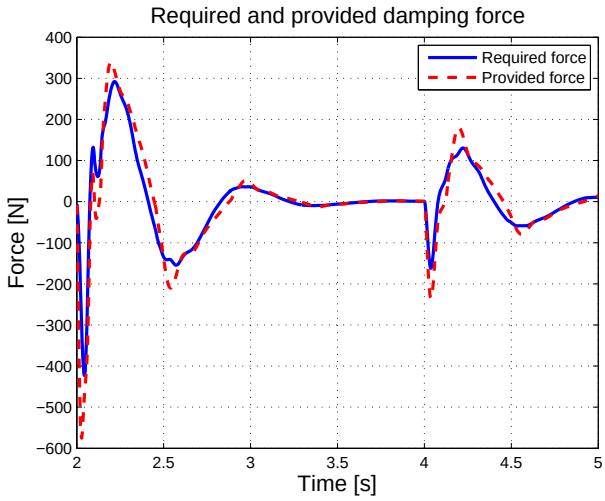

Fig. 11. Damping force control

the force actually provided are superposed. It means on the one hand that the required force was semi-active and on the other hand that this force was reachable, because the damper simulated has been able to follow the force reference. The performance of the force controller is also illustrated with the results of Figure 11.

V. CONCLUSIONS AND FUTURE WORKS

In this paper, an identified nonlinear static model of the damper and its actuator have been developed using experiment results. Then a $\mathcal{H}_\infty/LPV$ static state-feedback controller was synthesized using a linear quarter car model to compute the required damping force that minimizes given performance criteria. As this control strategy leads to an active force which is unreachable with such a semi-active damper, a scheduling parameter has been introduced to avoid the required force reference to be active. This parameter allows the controller to decrease the performance objectives if the required force is not in the reachable force range given by the identified model. The abilities of the real damper are considered in the controller. Then a local controller is used

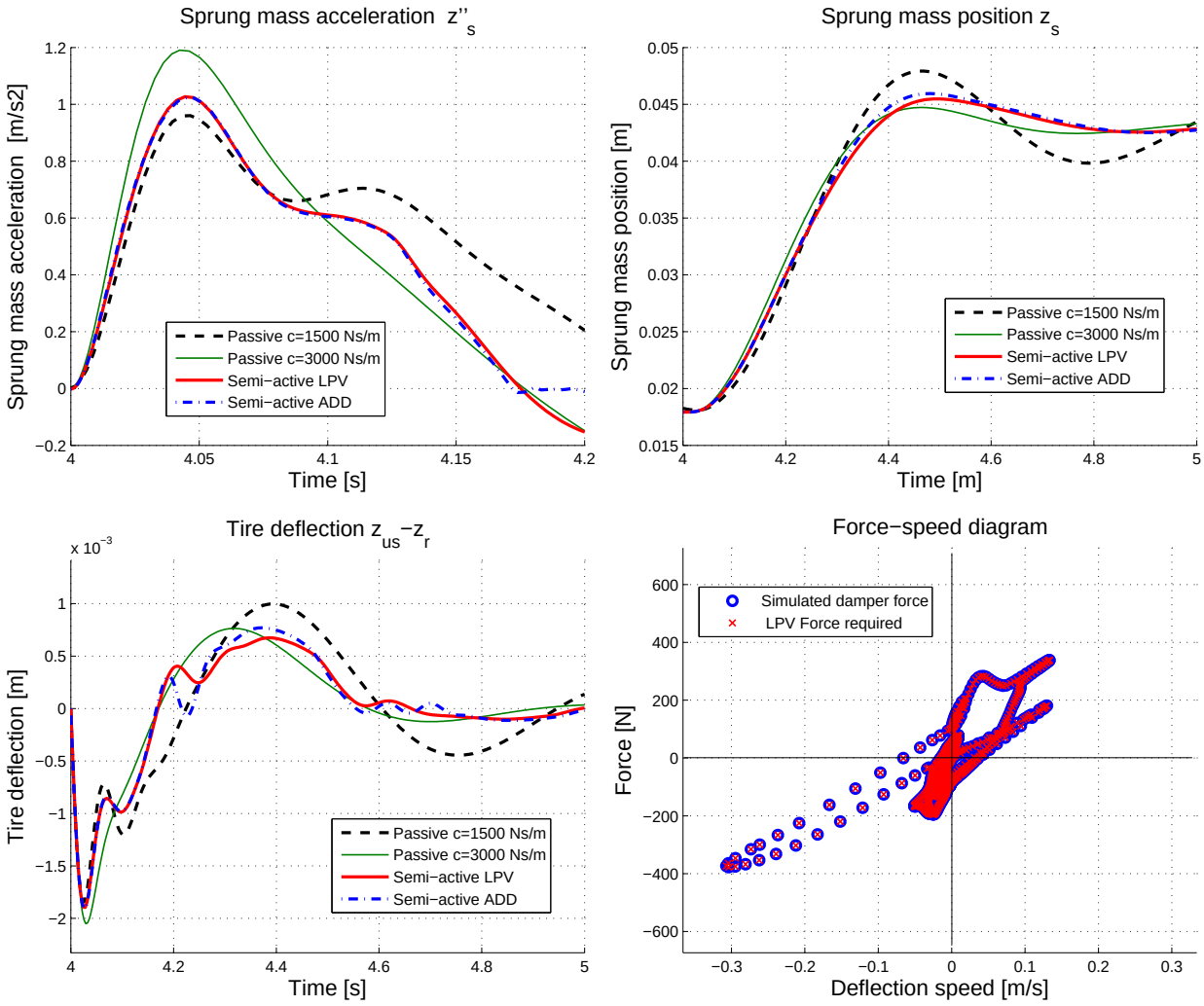

Fig. 10. Time results

to control the servomechanism and regulate the damping rate so that the damper provides the required force. Therefore the proposed control architecture includes a global control of the vehicle behavior and a local control of the servomechanism based on the real damping force. The results presented emphasize the performance improvement of the proposed control strategy in terms of comfort and safety.

Future works will consist in implementing and testing this control strategy with SOBEN on a testing car. Then a global attitude control strategy using the four suspensions will be developped and implemented.

REFERENCES

[1] E. Abdellahi, D. Mehdi, and M. M. Saad, "On the design of active suspension system by $\mathcal{H}_\infty$ and mixed $\mathcal{H}_2/\mathcal{H}_\infty$: An LMI approach," in *Proceedings of the American Control Conference*, Chicago, USA, june 2000, pp. 4041–4045.

[2] P. Apkarian, P. Gahinet, and G. Beker, "Self-scheduled $\mathcal{H}_\infty$ control of linear parameter-varying systems: A design example," *Automatica*, pp. 31(9), 1251–1262, 1995.

[3] S. Aubouet, O. Sename, B. Talon, C. Poussot-Vassal, and L. Dugard, "Performance analysis and simulation of a new industrial semi-active damper," in *Proceedings of the* $17th$ *IFAC World Congress*, Seoul, Korea, july 2008.

[4] M. Canale, M. Milanese, and C. Novara, "Semi-active suspension control using "fast" model-predictive techniques," in *IEEE Transactions on control systems technology, vol. 14,no. 6*, november 2006.

[5] S.-B. Choia, H. Leea, and E. Chang, "Field test results of a semi-active suspension system associated with skyhook controller," *Mechatronics*, pp. 11, 345–353, 2000.

[6] I. Fialho and G. Balas, "Road adaptive active suspension design using linear parameter varying gain scheduling," in *IEEE Transaction on Systems Technology*, january 2002, pp. 10(1),43–54.

[7] P. Gaspar, I. Szaszi, and J. Bokor, "Active suspension design using LPV control," in *Proceedings of the 1st IFAC Symposium on Advances in Automotive Control*, Salerno, Italy, 2004, pp. 584–589.

[8] N. Giorgetti, A. Bemporad, H. Tseng, and D. Hrovat, "Hybrid model predictive control application toward optimal semi-active suspension," *International Journal of Robust and Nonlinear Control*, pp. 79(5), 521–533, 2006.

[9] D. Karnopp, "Semi-active control of wheel hop in ground vehicles," *Vehicle System Dynamics*, pp. 12(6),317–330, 1983.

[10] T. Kawabe, O. Isobe, Y. Watanabe, S. Hanba, and Y. Miyasato, "New semi-active suspension controller design using quasi-linearization and frequency shaping," *Control Engineering Practice*, pp. 6, 1183–1191, 1998.

[11] C. Poussot-Vassal, "Robust multivariable linear parameter varying automotive global chassis control," PhD Thesis (in English), Grenoble INP, GIPSA-lab, Control System dpt., Grenoble, France, September 2008.

[12] C. Poussot-Vassal, O. Sename, L. Dugard, P. Gáspár, Z. Szabó, and

J. Bokor, “New semi-active suspension control strategy through LPV technique,” *Control Engineering Practice*, vol. 16, no. 12, pp. 1519–1534, December 2008.

[13] D. Sammier, O. Sename, and L. Dugard, “Skyhook and $\mathcal{H}_\infty$ control of active vehicle suspensions: some practical aspects,” *Vehicle System Dynamics*, pp. 39(4):279–308, April 2003.

[14] S. M. Savaresi, E. Siciliani, and S. Bittanti, “Acceleration driven damper: an optimal control algorithm for comfort oriented semi-active suspensions,” pp. 127(2), 218–229.

[15] C. Scherer and S. Weiland, *LMI in control (lecture support, DELFT University)*, 2004.

[16] C. Sherer, P. Gahinet, and M. Chilali, “Multiobjective output-feedback control via lmi optimization,” in *IEEE Transaction on Automatic Control*, july 1997, pp. 42(7):896–911.

[17] S. Y. Shuqi Guo and C. Pan, “Dynamic modeling of magnetorheological damper behaviors,” *Journal of Intelligent Material Systems and Structures*, pp. 17, 3, 2006.

[18] C. Spelta, “Design and applications of semi-active suspension control systems,” Phd Thesis, Politecnico di Milano, dipartimento di Elettronica e Informazione, 2008.

[19] R. Takahashi, J. Camino, D. Zampieri, and P. Peres, “A multiobjective approach for $\mathcal{H}_2$ and $\mathcal{H}_\infty$ active suspension control,” in *Proceedings of the American Control Conference*, Philadelphia, USA, june 1998, pp. 48–52.

[20] H. Tseng and J. Hedrick, “Semi-active control laws: optimal and sub-optimal,” *Vehicle System Dynamics*, pp. 23(1), 545–569, 1994.

[21] K. Yi and B. S. Song, “Observer design for semi-active suspension control,” *Vehicle System Dynamics*, pp. 32, 129–148, 1999.

[22] A. Zin, “Sur la commande robuste de suspensions automobiles en vue du contôle global de chassis,” Phd Thesis, Institut National Polytechnique de Grenoble, 2005.